Powder Metallurgy

ISSN: (Print) (Online) Journal homepage: https://www.tandfonline.com/loi/ypom20

High-speed formation of a near-full-density bondline in sinter-bonding below 250°C using 2 μm Cu particles coated with Ag

Sung Yoon Kim , Eun Byeol Choi , Dong-Hyun Joo & Jong-Hyun Lee

To cite this article: Sung Yoon Kim , Eun Byeol Choi , Dong-Hyun Joo & Jong-Hyun Lee (2020) High-speed formation of a near-full-density bondline in sinter-bonding below 250°C using 2 μm Cu particles coated with Ag, Powder Metallurgy, 63:5, 367-380, DOI: 10.1080/00325899.2020.1820664

To link to this article: https://doi.org/10.1080/00325899.2020.1820664

Published online: 16 Sep 2020.

POWDER METALLURGY
2020, VOL. 63, NO. 5, 367–380
https://doi.org/10.1080/00325899.2020.1820664

The Institute of Materials, Minerals and Mining
Taylor & Francis
Taylor & Francis Group

High-speed formation of a near-full-density bondline in sinter-bonding below 250°C using 2 μm Cu particles coated with Ag

Sung Yoon Kim[a], Eun Byeol Choi[b], Dong-Hyun Joo[c] and Jong-Hyun Lee [a]

[a]Department of Materials Science and Engineering, Seoul National University of Science and Technology, Seoul, Republic of Korea; [b]Program of Materials Science and Engineering, Convergence Institute of Biomedical Engineering and Biomaterials, Seoul National University of Science and Technology, Seoul, Republic of Korea; [c]Convergence Institute of Biomedical Engineering and Biomaterials, Seoul National University of Science and Technology, Seoul, Republic of Korea

ABSTRACT

High-speed attachment of dies on an Ag finish was demonstrated through pressure-assisted sinter-bonding at temperatures <250°C using 2 μm Cu particles coated with Ag, to achieve a high-temperature sustainable bondline. The Ag shells were dewetted by instability at the Ag layer/Cu core interface during heating, which initiated the sinter-bonding. Consequently, in the case where Ag coating content was 20 wt-%, sufficient shear strengths of 24.6 and 34.1 MPa were measured even after an extremely short bonding time of just 1 min, at 220 and 250°C, respectively. When Ag coating content was increased to 40 wt-%, high shear strengths of 29.5–30.5 and 35.6–36.3 MPa were measured after ultra-rapid bonding for 0.5–1 min at 220 and 250°C, respectively. Furthermore, near-full-density bondlines could be achieved through a nano-volcanic eruption behaviour after a relatively short bonding time of 5 min at both 220 and 250°C.

ARTICLE HISTORY
Received 16 March 2020
Accepted 31 August 2020

KEYWORDS
Sinter-bonding; die attachment; Ag-coated Cu particle; Ag dewetting; full density; shear strength

1. Introduction

Following the expansion of the electronic industry, different solder alloys have been developed mainly for the bonding and mounting of various devices and parts [1–11]. Although soldering enables many components to be simultaneously bonded within a relatively short time [9,10], some unresolved problems still remain in its application in various fields. A typical drawback is the low melting point of solders that leads to reliability issues such as re-melting or a significant reduction in mechanical properties in applications where the bonding material is exposed to high temperature [5,6]. High-temperature solder alloys containing excess Pb also have constraints at working temperatures approaching 300°C and could be subject to a ban with respect to the use of Pb [4,5,11]. Another notable drawback of solders is their low thermal conductivity, which severely accelerates thermal degradation of heat-sensitive parts [2,4,6,7].

The continuous pursuit of methods to form the high-temperature sustainable bondline has motivated studies to develop novel bonding techniques. Recently, the sinter-bonding technique by substituting the bonding material by silver particles is being explored and is a hot research topic owing to the high re-melting point, extremely high thermal conductivity and the advantageous mechanical ductility of Ag [12–23]. Nevertheless, there are serious problems in the sinter-bonding of Ag particles, as described in the following: as the bonding proceeds by normal sintering, bonding time is inherently longer when compared with soldering [13,14,17,23]. The formation of near-full-density bondlines by the sintering can be accelerated by using entirely or greater quantities of nanoparticles [19–22], which increases cost. However, since near-full-density samples contain only tiny voids, the initiation and propagation of cracks in the bondline can be effectively suppressed, thus enhancing the reliability of the joint [16,20,22]. Finally, the high cost of Ag is the biggest problem in the industrial use of such processes.

A novel sinter-bonding technique using Ag-coated Cu (Cu@Ag) particles was developed in this study to simultaneously solve the above-mentioned three problems. The particle size of the Cu particles was several micrometre and the thickness of the Ag shell was varied in the range from 100 nm to several hundreds of nanometres. As a result, the material cost is significantly reduced when compared with pure Ag particles. The novel sinter-bonding technique was performed with assistance of high external pressure to simultaneously obtain both high sinter-bonding speed and near full density at the bonding temperatures of 220 and 250°C, which are lower than previously reported sinter-bonding temperatures and are similar to the peak temperatures in Pb-free soldering processes [7,8,11].

CONTACT Jong-Hyun Lee pljh@snut.ac.kr Department of Materials Science and Engineering, Seoul National University of Science and Technology, Seoul, Republic of Korea

2. Experimental procedures

2.1. Powder preparation

In the preparation of particles with core–shell structure to induce microstructural changes in Ag shells during sinter-bonding, spherical Cu particles were chosen as the core material. Spherical Cu particles (average size: 2 μm) were purchased from CNVISION Co., Ltd. Cu particles (3 g) were immersed into a pretreatment solution and stirred at 200 rpm for 2 min at room temperature (RT) to remove the oxide layer from the surface. The pretreatment solution was prepared by dissolving 2.090 M of ammonium sulphate ($(NH_4)_2SO_4$, 99%, Samchun Pure Chemical Co., Ltd) and 150 mM of ammonium hydroxide (NH_4OH, 28–30%, Samchun Pure Chemical Co., Ltd) in 100 ml of deionised (DI) water. After the pretreatment, the Cu particles were washed three times with DI water and maintained in suspension by dispersing in 100 ml DI water.

The Ag plating solution was made by dissolving 3.560 M of NaOH (97.0%, Daejung Chemicals & Metals Co., Ltd), 0.890 M of ethylenediaminetetraacetic acid (EDTA, $C_{10}H_{16}N_2O_8$, 99.0%, Samchun Pure Chemical Co. Ltd), and silver nitrate ($AgNO_3$, 99.8%, Hojeonable Inc.) in 100 ml of DI water. Two Ag plating solutions were prepared where 0.055 and 0.110 M of silver nitrate was dissolved to prepare plating solutions containing of 20 and 40 wt-% of Ag with respect to the Cu powder content. The Ag plating solution was added dropwise into the Cu solution at the rate of 10 mL/min under continuous stirring at RT, after which, the mixed solution was stirred at the rate of 250 rpm for 5 min to complete the Ag coating reaction. The fabricated Cu@Ag particles were washed twice successively with DI water and methyl alcohol (95%, Hanwha Chemical Co.) and then dried at RT in a vacuum chamber.

2.2. Sinter-bonding

Pastes containing Cu@Ag particles were prepared by mixing with α-terpineol (98.5%, Samchun Chemical Co., Ltd) as the vehicle. The particle-to-vehicle weight ratio was adjusted to 85:15 to obtain appropriate viscosity. Test dies for die attachment tests were prepared using a dummy Cu plate of dimensions 3 × 3 × 1 mm^3, finished with an ~0.2 μm thick Ag layer. The Ag finishes were formed by electroless plating on the Cu plates and in some cases, the layer thickness increased to 1 μm. Alumina-based DBC substrates (10 × 10 × 1 mm^3) also containing Ag finishes of 1 μm thickness were used. The prepared paste was printed on the Ag-finished substrate through a stencil mask with a slit volume of 3 × 3 × 0.1 mm^3. After printing, the die was placed under aligning on the printed pattern and the resulting sandwich-structures were heated to 220 or 250°C; the heating rate was ~6.25°C/s in both cases. The die bonding was conducted in air under 80 MPa pressure, which was maintained for the entire bonding time.

2.3. Characterisation

The shape and surface morphology of the fabricated Cu@Ag particles and the microstructures of the bondlines and fracture surfaces were observed using a high-resolution scanning electron microscope (HR-SEM, SU8010, Hitachi). Phase characterisation of the fabricated Cu@Ag particles was performed by using X-ray diffraction (XRD, DE/D8 Advance, Bruker). Element identification in the cross-section of a Cu@Ag particle was performed using energy-dispersive X-ray spectroscopy (EDS, NORAN SYSTEM 7, Thermo Scientific). The bonding strength of the bondline was determined from the maximum stress value measured during shear testing of the bonded die with a shear height of 200 μm at 200 μm/s using a bond-tester (Dage-4000, Nordson Dage).

3. Results

3.1. Ag-coated Cu particles

Figure 1 shows the Cu particles with an average size of 2 μm used in this study. Although the particle size has a distribution in the 1.1–2.3 μm range, all the particles have a smooth surface, since they were prepared by an atomisation process. SEM images of the Cu particles plated with different amounts of Ag are presented in Figure 2(a)–(d). The increase in Ag shell thickness due to an increase in Ag content is clearly confirmed from the cross-sectional back-scattered electron (BSE) images. While the average thickness of the Ag shell fabricated with 20 wt-% is 108 (±30) nm, that of the shell formed with 40 wt-% is 256 (±56) nm. A more direct evidence of the morphology change is observed in the surface images. As the Ag content is increased, the shell surface becomes rougher [24]. Moreover, intensities of Ag peaks in the XRD result (Figure 2(e)) increased with an increase in the average thickness of the Ag shell.

3.2. Sinter-bonding using 20 wt-% Ag-coated Cu particles

Figure 3 shows the upper and lower bondline microstructures of Ag-finished dummy dies sinter-bonded at 220°C using 20 wt-% Ag-coated Cu particles. For the samples sinter-bonded for just 0.5 min (30 s), slight sintering among the Ag shells at the contacts between the particles is observed. However, sintering is scarcely observed, both at the upper interface between Cu@Ag particles and the Ag finish of the die, and the lower

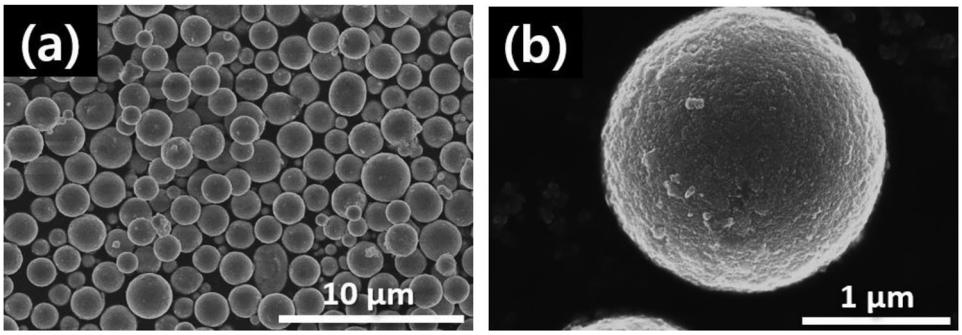

Figure 1. (a) Low- and (b) high-magnification SEM images of the 2 µm Cu particles used in this study.

interface between the Cu@Ag particles and the Ag finish of the substrate, except for a few sintered particles on the finishes. In particular, continuous detachment was observed at the upper interfaces of the samples after mounting and polishing, indicating poorer bonding capability at this interface than that at the lower interface with a thicker Ag finish, which has a better contact due to the effect of gravity. Even when the bonding time was increased to 1 min, continued detachment at the upper interface was still observed due to the insufficient sintering time, but the uniformity of packing among the Cu@Ag particles was enhanced. However, when the bonding time was increased to 5 min, a slight sinter-bonding was

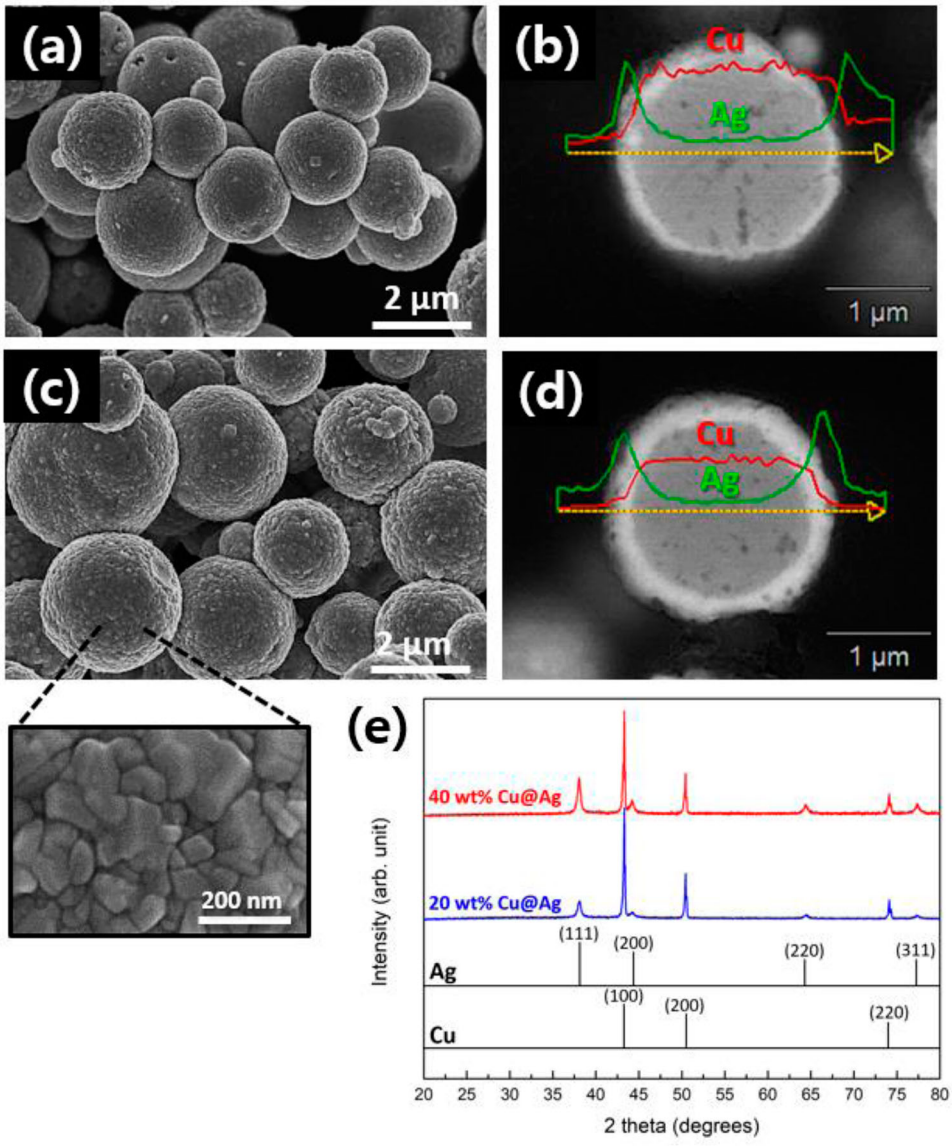

Figure 2. (a,c) Surface SEM images and (c,d) cross-sectional BSE images and line profiles of Cu@Ag particles with different Ag contents: (a,b) 20 and (c,d) 40 wt-%. (e) XRD results of powder.

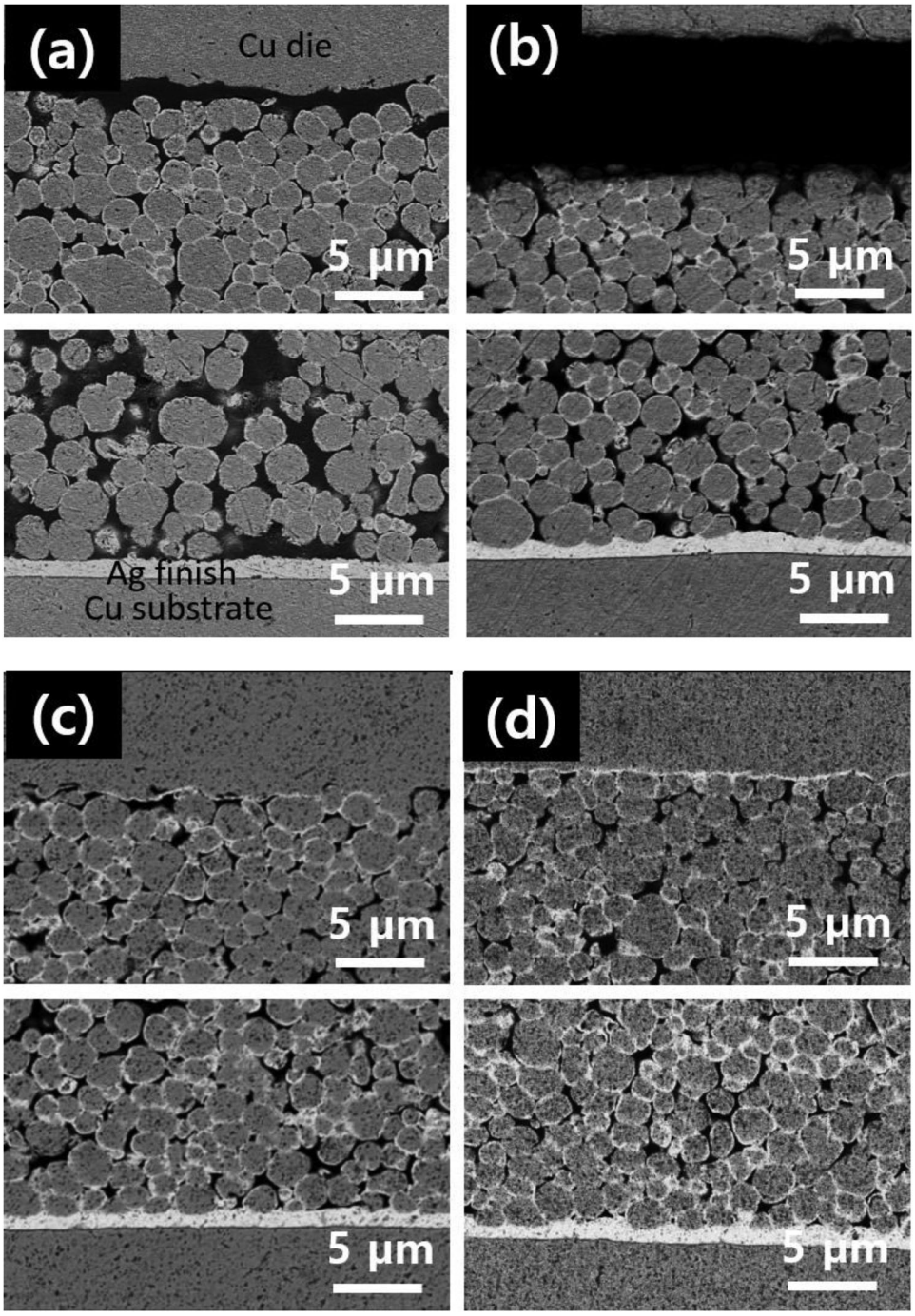

Figure 3. Cross-sectional BSE images showing upper and lower bondlines of Ag-finished dies sinter-bonded at 220°C using 20 wt-% Ag-coated Cu particles for (a) 0.5, (b) 1, (c) 5, and (d) 10 min.

observed between the Cu@Ag particles and the Ag finish of a die at the upper interface and the sintering between Ag shells on the particles was also evidently enhanced, although voids still remained between the particles. In the case where the samples were bonded for 10 min, sinter-bonding at the upper interface was stronger accompanied by a decrease in voids between the particles.

To achieve faster sinter-bonding by forming an effective bond at the Ag finish/particle interface and to obtain a dense bondline, the bonding temperature was increased by 30–250°C. The cross-sectional bondline images of Ag-finished dies sinter-bonded at 250°C are displayed in Figure 4. For the samples sinter-bonded for just 0.5 min, there was very little sintering at the upper interface between the Cu@Ag particles and the Ag finish of the die, when compared with that between the particles, as well as that at the lower interface between the Cu@Ag particles and the Ag finish of the substrate. However, with the longer bonding time of 1 min, the sintering at the upper interface was observed to be slightly reinforced, although the sintering between Cu@Ag particles was still not sufficient. When the bonding time was increased to 5 min, both the sintering at the upper interface and between the particles were further improved. Lastly, sintering between the particles was

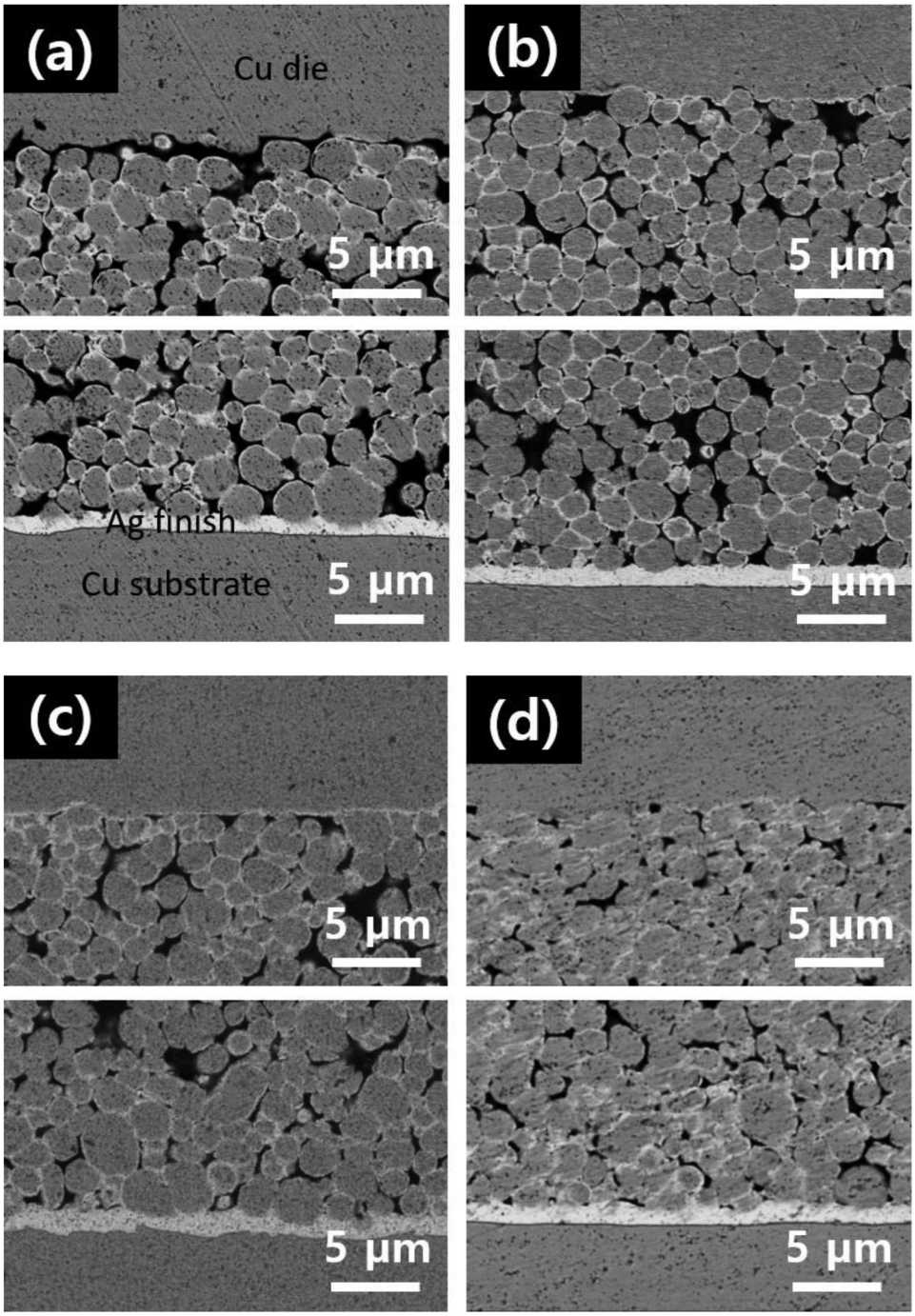

Figure 4. Cross-sectional bondline BSE images of Ag-finished dies sinter-bonded at 250°C using 20 wt-% Ag-coated Cu particles for (a) 0.5, (b) 1, (c) 5 and (d) 10 min.

strikingly enhanced after bonding for 10 min, resulting in a reduced void fraction. In summary, the 30°C increase to 250°C generally enhanced sintering between Cu@Ag particles and the Ag finish, as well as between the Cu@Ag particles.

Continued detachment at the upper interface observed after short bonding intervals of 0.5–1 min at 220°C indicated inadequate sintering between Cu@Ag and the Ag finish on a die due to the low Ag content at the interface. Thus, similar bonding tests were conducted with dummy dies where the Ag finish thickness was increased to 1 µm, and the cross-sectional bondline images of these samples are shown in Figure 5. Under these conditions, the samples (Figure 5(a)) sinter-bonded for 0.5 min at 220°C using 20 wt-% Ag-coated Cu particles revealed detachment at the inside of the bondline after the mounting and polishing, which was inconsistent with Figure 3 (a). Thus, the upper interface reinforced with a thick Ag finish induced crack propagation along the weakest points in the degree of sinter-bonding (the interface between Ag-coated Cu particles). When increasing the bonding time to 1 min, the sinter-bonding at the upper interface is found to be enhanced to a greater degree together with a slight improvement in inter-particle sintering, as shown in Figure 5(b).

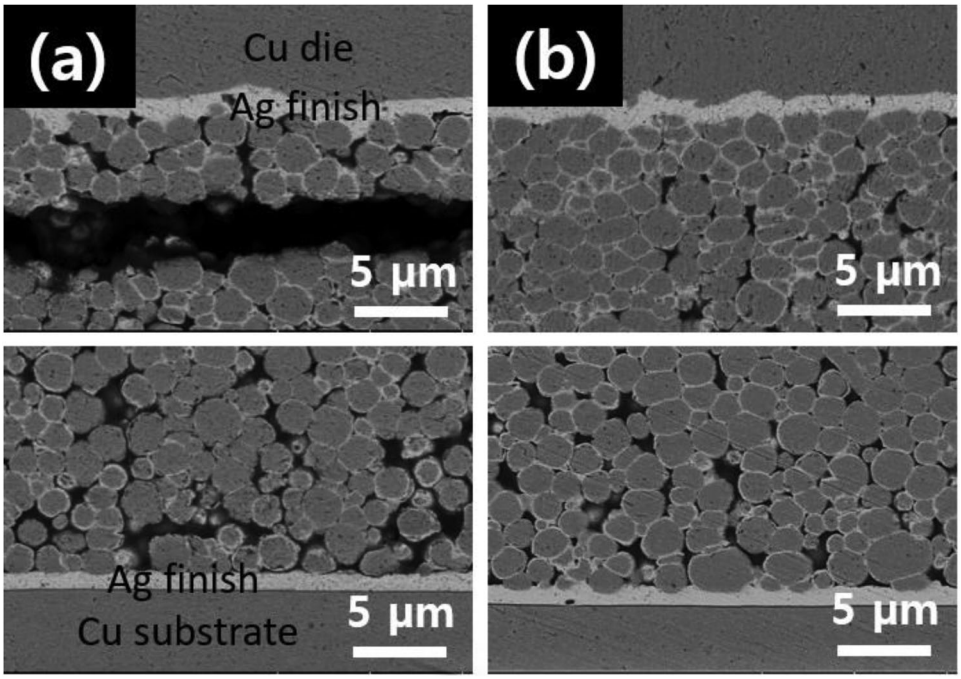

Figure 5. Cross-sectional bondline BSE images of Ag-finished dies sinter-bonded at 220°C using 20 wt-% Ag-coated Cu particles for (a) 0.5 and (d) 1 min, when the thickness of the Ag finish on the dies was increased to 1 μm.

Figure 6 shows a plot of the shear strength of dies sinter-bonded as a function of bonding temperature and time when using Cu@Ag particles with 20 wt-% Ag shell. It is seen that regardless of the temperature, the strength is increased with an increase in bonding time. For bonding at 220°C, the strength values for the dies bonded for a short time such as 1 min are found to be insufficient. However, when bonded for 5 min, the strength exceeded 20 MPa and reached a very high value of 46.1 MPa after 10 min. When the bonding temperature was increased to 250°C, the strength obtained for a very fast bonding time of 0.5 min was 15.2 MPa. However, the strength exceeded 30 MPa (34.1 MPa) even after a still short bonding time of 1 min. This value is higher than that measured after 60 min bonding at an identical temperature when using hybrid Ag paste [23]. Moreover, the strength increased up to greatly high values of 55.0 and 64.7 MPa for increased bonding times of 5 and 10 min, respectively. When the Ag finish thickness was increased to 1 μm, the strength was significantly enhanced, attaining a satisfactory value of 24.6 MPa even with a very short bonding time of 1 min. This value is higher than that measured for samples bonded using high Pb solder paste [11]. Furthermore, the strengths were still slightly higher than those of samples bonded for 5 min using dies with low thickness of Ag finish.

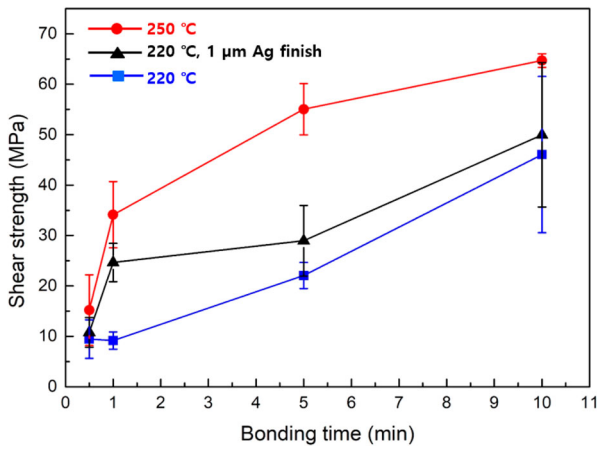

Figure 6. Shear strength of dies sinter-bonded at different temperatures for different times using a paste containing Cu@Ag particles with Ag shell content of 20 wt-%.

The fracture surfaces observed after the shear test are displayed in Figures 7–9. Figure 7 shows the fracture surfaces of the dies bonded at 220°C, as a function of the bonding time. After short bonding times of 0.5 and 1 min, a fracture is seen along the interface between the Ag finish of a die and the Cu@Ag particles, indicating interface failure. Thus, large fractions of the fracture surfaces on the bondlines show scarcely any sintering between the particles and very small areas where sintering had occurred. However, the facture surface changed from the upper interface to the inside of the bondline for bonding time of 5 min, indicting a coherent failure. Moreover, in the samples bonded for 5 min, significantly enhanced sintering between the particles was observed on the whole at the fracture surface. These microstructural characteristics are in good accordance with results observed in Figure 3. Ductile striations, which can be formed on the well-sintered structure during shear test, are also observed. With an increase in the bonding time to 10 min, it was observed that both sintering and formation of ductile striations were intensified.

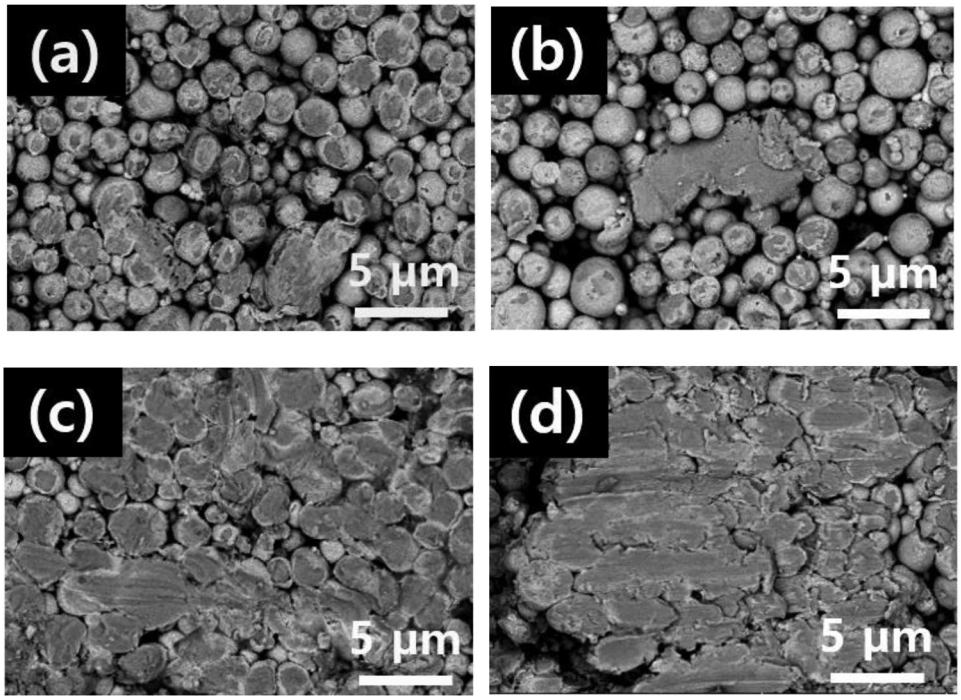

Figure 7. Fracture surface BSE images of bondlines fabricated at 220°C with different bonding times when the thickness of Ag finish is 0.2 µm: (a) 0.5, (b) 1, (c) 5 and (d) 10 min.

With an increase in thickness of Ag finish on the die to 1 µm, all fracture modes were transformed into coherent fractures (Figure 8). Nevertheless, severe sintering between the Ag-coated Cu particles was not observed in the fracture surface on a bondline after 0.5 min bonding. However, the degree of sintering was strikingly enhanced even with a slight increase in bonding time to 1 min. These characteristics of the fracture surface clearly account for the abrupt increase in strength after 1 min bonding shown in Figure 6.

Fracture surfaces of the samples bonded at 250°C are presented in Figure 9. Similar to previous results, abundant sintering between the particles is observed in large areas of the sample bonded for 1 min, while the sintering occurred only locally in the sample bonded for 0.5 min. Hence, the interface failure at the upper interface of the samples bonded for 0.5 min changed to coherent failure in the samples bonded for 1 min. This microstructural characteristic clearly justifies the abrupt strength increase of the 1 min samples in Figure 6. The area characterised by sintering increased with an increase in bonding time to 5 min, and sintering was observed in most areas of the fracture surface when the time was increased to 10 min.

3.3. Sinter-bonding using 40 wt-% Ag-coated Cu particles

Figure 10 shows the upper and lower bondline microstructures of Ag-finished dies sinter-bonded at 220°C using 40 wt-% Ag-coated Cu particles. In the sample sinter-bonded for just 0.5 min, a partial sintering among the Ag shells at the contacts between the particles is observed, which, however, failed to cover a maximum of the total sintered area. When the bonding time was increased to 1 min, the sintering among Ag shells was slightly enhanced and increased bonding area per particle was observed. With further increase in bonding

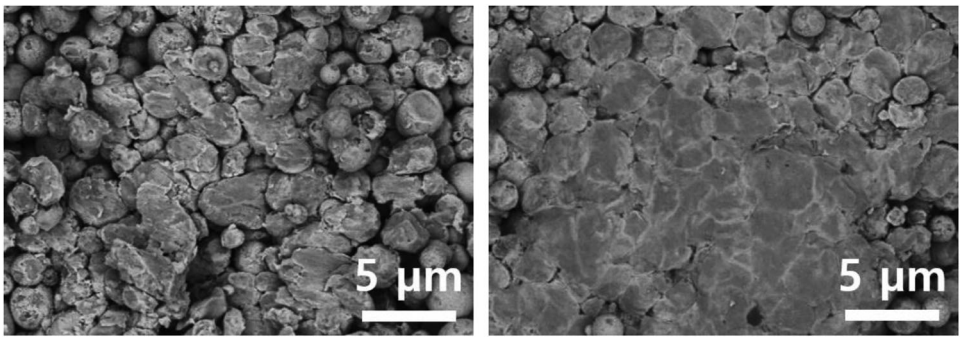

Figure 8. Fracture surface BSE images of bondlines fabricated at 220°C for (a) 0.5 and (b) 1 min for samples where the thickness of Ag finish is increased to 1 µm.

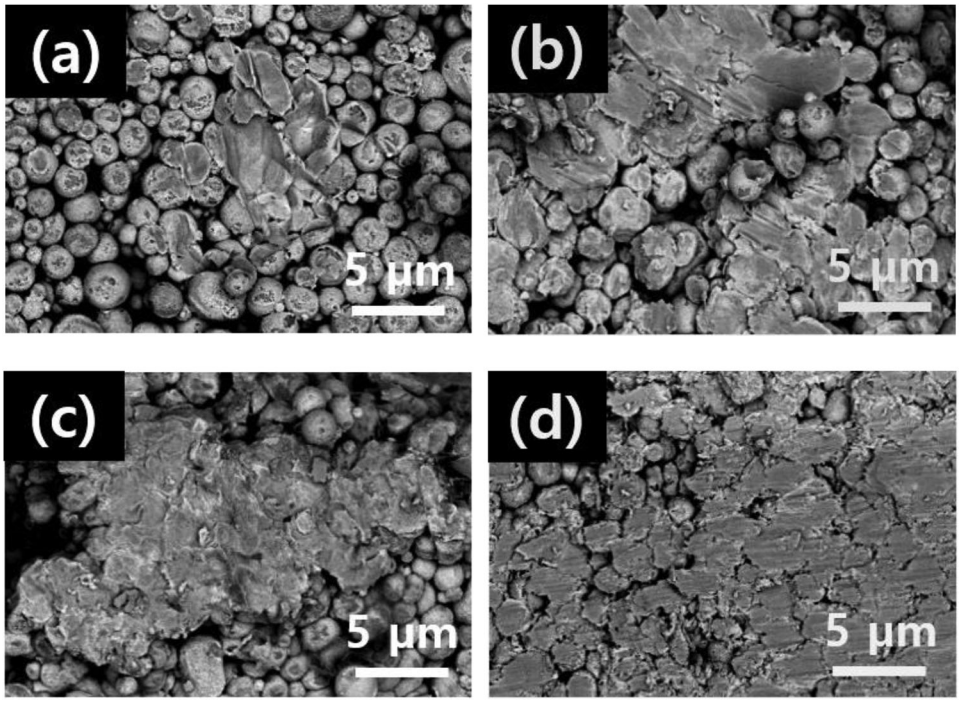

Figure 9. Fracture surface BSE images of bondlines fabricated at 250°C with different bonding times; the thickness of the Ag finish is 0.2 μm: (a) 0.5, (b) 1, (c) 5 and (d) 10 min.

time to 5 min, however, a significantly different bondline microstructure with near full density was observed, together with the complete sinter-bonding at the interfaces. With an increase in bonding time up to 10 min, the tiny voids in the bondline nearly disappeared.

To achieve even higher-speed sinter-bonding, the bonding temperature was changed to 250°C. The upper and lower bondline microstructures of Ag-finished dies sinter-bonded with an increase in the bonding temperature by 30°C using 40 wt-% Ag-coated Cu particles are displayed in Figure 11. In the samples sinter-bonded for just 0.5 and 1 min, the voids between the particles still existed, although the sinter-bonding at the upper and lower interfaces as well as the sintering between the Cu@Ag particles were definitely enhanced. However, most of the voids disappeared and the sintering at the interfaces seemed to be complete when the bonding time was increased to 5 min. With further increase in bonding time to 10 min, the bondline became a tightly sintered structure. In summary, pronounced interface sinter-bonding and near-full-density bondline were attained just after 0.5 and 5 min, respectively, at the bonding temperature of 250°C using 40 wt-% Ag-coated Cu particles.

Figure 12 shows the shear strength of dies sinter-bonded at different bonding temperatures and for different times using Cu@Ag particles with 40 wt-% Ag shell. For both the bonding temperatures, strength increased with increasing bonding time. Moreover, the strengths at 250°C are higher than those at 220°C for all measured bonding times. As a result, the average strength of the dies sinter-bonded just for 0.5 min at 250°C exceeded 35.0 MPa (35.6 MPa), which is higher than that measured after 60 min bonding using hybrid Ag paste [23]. In addition, the die bonded for 5 min showed an unusually high strength of 68.4 MPa. These excellent strength values are attributed to the extremely high density of the microstructure in the bondlines. In summary, shear strengths exceeding 34.0 MPa after sinter-bonding at 250°C could be attained after a 1 min bonding process for 20 wt-% Ag shells and using the 0.5 min process for 40 wt-% Ag shells, respectively, which are extremely rapid when compared with previous results.

The fracture surfaces observed after the shear test of bondlines fabricated at 220 and 250°C with different bonding times are displayed in Figures 13 and 14. All the fractures were characterised as coherent fractures. In the fracture surfaces of 220°C bonding (Figure 13), a locally sintered microstructure was observed just after an extremely short bonding time of 0.5 min, and the total sintered area expanded in proportion to the prevalence of ductile striations as the bonding time was increased up to 10 min. In the fracture surfaces of the bondline formed at 250 °C (Figure 14), developed ductile striations were found in the fairly sintered bondline even after a short bonding time of 0.5 min. The degree of sintering and ductile striation formation in the fractured surfaces increased with an increase in bonding time.

To achieve the near-full-density bondline at 220°C using lower pressures, the sinter-bonding for 5 min using 40 wt-% Ag-coated Cu particles was finally performed under different external pressures, as shown in Figure 15. Owing to the large interparticulate voids created by the mono-sized 2 μm size particles, the near full density was obtained even after 70 MPa

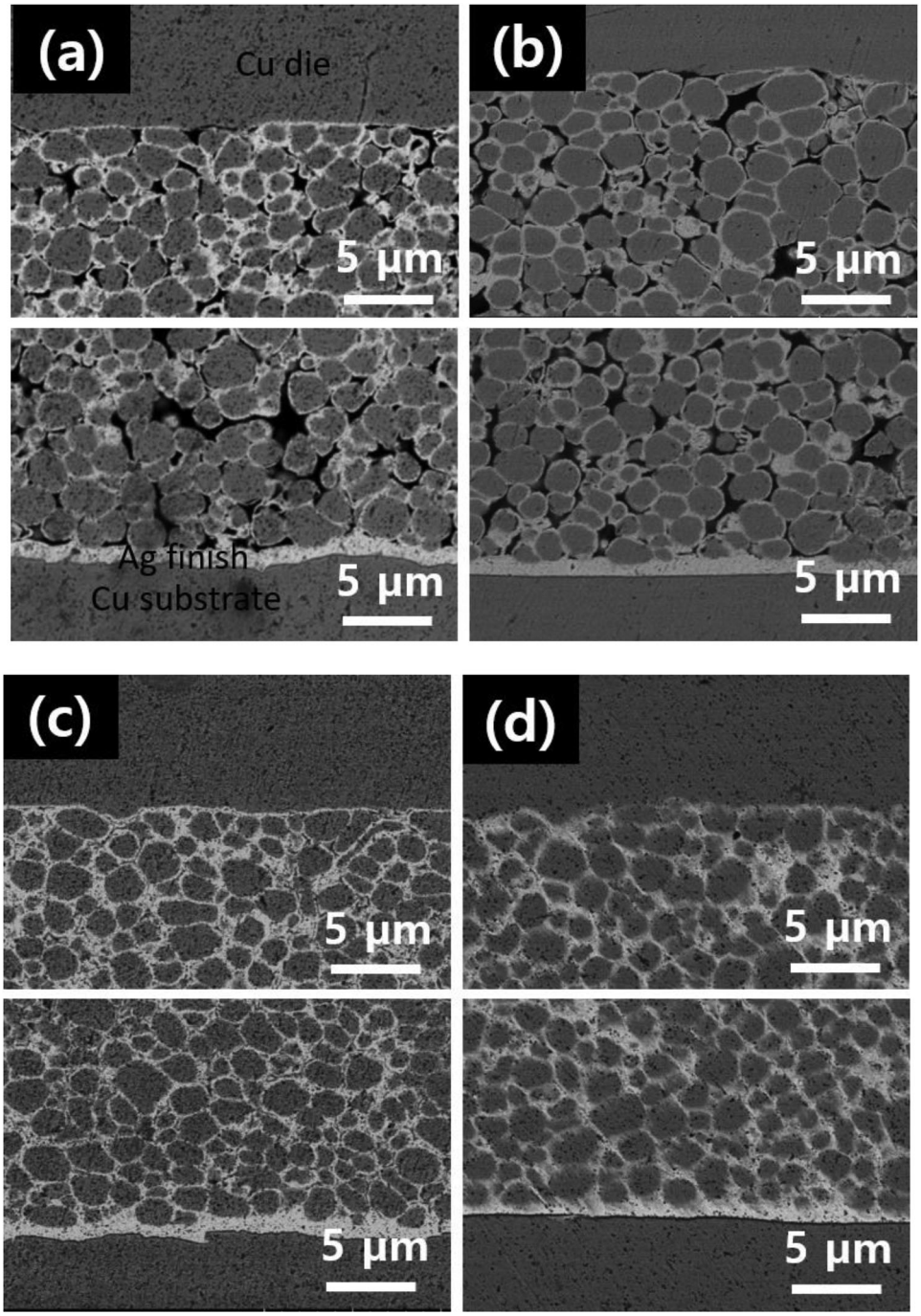

Figure 10. Cross-sectional BSE images showing upper and lower bondlines of Ag-finished dies sinter-bonded at 220 °C using 40 wt-% Ag-coated Cu particles for (a) 0.5, (b) 1, (c) 5 and (d) 10 min.

pressing. The shear strengths after the 50, 60 and 70 MPa pressing were measured to be 22.6, 26.8 and 41.0 MPa, respectively. Therefore, to achieve the near full density and the rapid increase in shear strength more efficiently under relatively low external pressures such as 10 MPa, enhancement of the initial packing density by using the bimodal-sized particles is required [19–21,23].

4. Discussion

The formation behaviour leading to a near-full-density bondline structure can be understood as follows. In the case where the average thickness of the Ag shell is low, e.g. from several to several tens of nanometres, the temperature at which the dewetting of the shell occurs depends on the size of Cu core particle due to the interfacial instability induced by the difference in lattice mismatch of 11.7% between Ag and Cu [25–28], irregularly forming tiny nodules on the Cu surface [24,29]. For 2 μm size Cu particles, initiation of dewetting is anticipated at ~220°C [24]. Comparing with the microstructure (Figures 3(b) and 10(b)) of the bondline sinter-bonded at 220°C for 1 min, the slightly enhanced sintering in the microstructure (Figures 4(b) and 11(b)) of the bondline sinter-

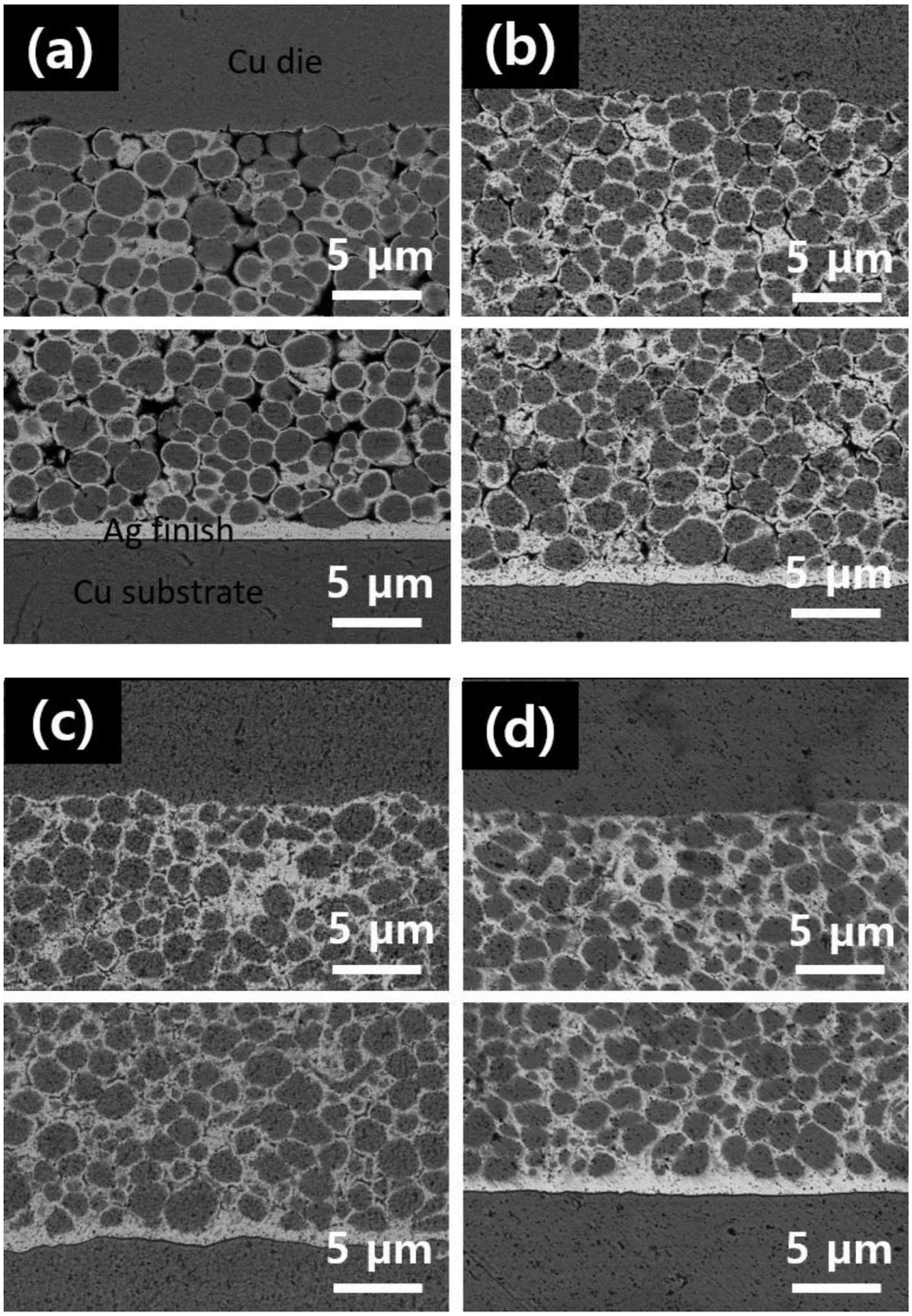

Figure 11. Cross-sectional bondline BSE images of Ag-finished dies sinter-bonded at 250°C using 40 wt-% Ag-coated Cu particles for (a) 0.5, (b) 1, (c) 5 and (d) 10 min.

bonded at 250°C for 1 min seems to be owing to Ag to Ag sintering by the dewetting behaviour of Ag shells. The Ag nano-nodules formed on the particle surfaces by the dewetting may enhance sinterability at the contacts between particles due to a more active surface, as shown in Figure 16. However, a high-density bondline microstructure was not observed when the Ag shells of low thickness were used. Hence, a different mechanism for the observed acceleration of sintering is needed to explain the near-full-density structure achieved when using a thick Ag shell.

When the thickness of the Ag shell is as high as several hundreds of nanometres as observed in the 40 wt-% Ag shell, the sizes of nodules generated on the top surface of a thick Ag shell resulting from dewetting do not increase in proportion to the thickness, and the nodule finally spreads outward becoming a more porous Ag layer [24]. Hence, the Ag dewetting behaviour cannot convincingly explain the rapid formation of near-full-density microstructure in the samples containing thick Ag shells (Figures 10 and 11). The unexpected fast annihilation of voids between particles in the sample of thick Ag shells can be accounted for by invoking a nano-volcanic eruption phenomenon [30–32]. In the grain-boundaries of a particle larger than a specific size,

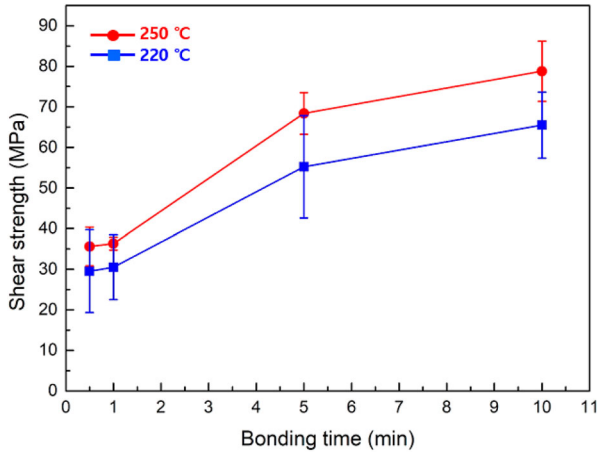

Figure 12. Shear strength of dies sinter-bonded at different bonding temperatures for different times using a paste containing Cu@Ag particles with 40 wt-% Ag shell.

the exposed Ag atoms combine with O atoms in air, forming Ag–O. The Ag–O compound (especially AgO) is thermodynamically more stable in the liquid state at the bonding temperature, which induces grain-boundary liquation and subsequently leads to a nano-volcanic eruption behaviour in the presence of compressive stress applied on the grain-boundaries, spouting tiny Ag and Ag_2O clusters, and O_2 gas [30]. Because the spouted Ag_2O also thermodynamically decompose to Ag at ~145°C [30], most of the spouted clusters finally transform into extremely small Ag nanoparticles with outstanding sinterability owing to the presence of an unstable surface or a liquid phase. The Ag nanoparticles of sizes in the range of several nanometres so formed would be in the liquid phase, as expected from the Gibbs–Thomson equation [33–36]. Consequently, the extremely small Ag nanoparticles generated from the thick shells would easily and quickly fill the voids between the Cu@Ag particles, changing the bondline structure into a much higher density structure. The formation of porous Ag layer via the outward spread of surface nodules observed in the separated thick Ag shell is also a result by a nano-volcanic eruption behaviour. Judging from previous sinter-bonding experiments performed with different particle sizes [29,31], the minimum particle size to easily induce a nano-volcanic eruption is anticipated to be in the scale of several hundreds of nanometres, which corresponds to the thickness attained by the 40 wt-% Ag shell in this study.

5. Conclusions

Bonding of Ag finish dies on Ag-finish substrate was performed through sintering at temperatures below 250°C under an external pressure of 80 MPa using 2 μm Cu particles coated with Ag to achieve a bondline with sustained mechanical stability even at temperatures much higher than 300°C. For the two Ag plating contents of 20 and 40 wt-%, the average thicknesses of the Ag shell were 108 and 256 nm, respectively. After mixing with α-terpineol, the obtained pastes were applied in sinter-bonding experiments. In bonding experiments, dewetting of the Ag shells occurred due to instability at the Ag layer/Cu core interface during heating, forming active nano-

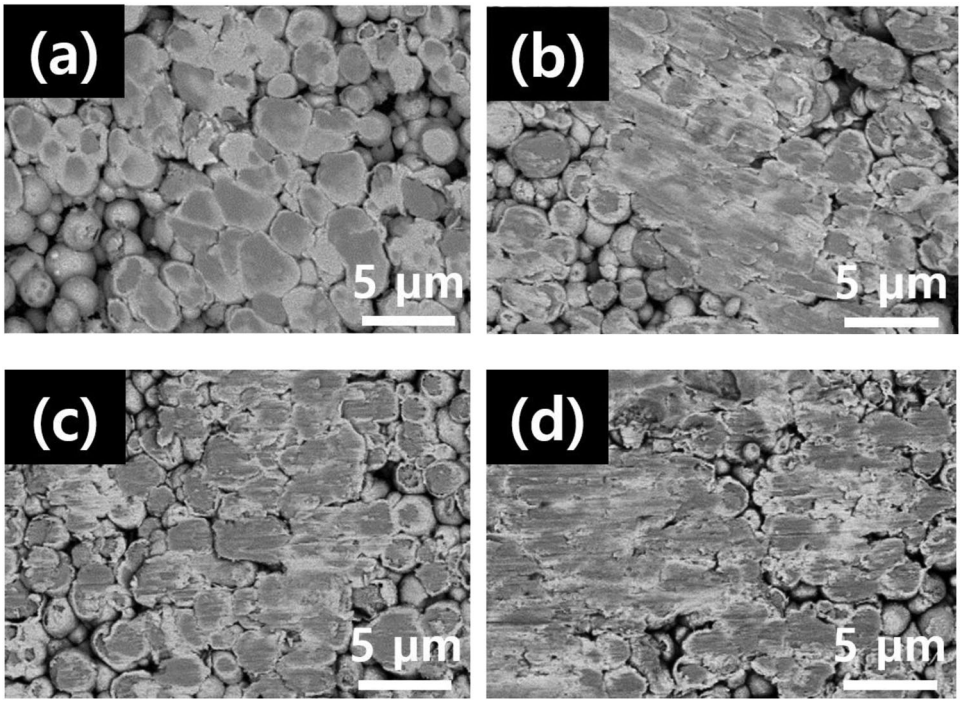

Figure 13. BSE images showing fracture surfaces of bondlines fabricated at 220°C using 40 wt-% Ag-coated Cu particles for different bonding times: (a) 0.5, (b) 1, (c) 5 and (d) 10 min.

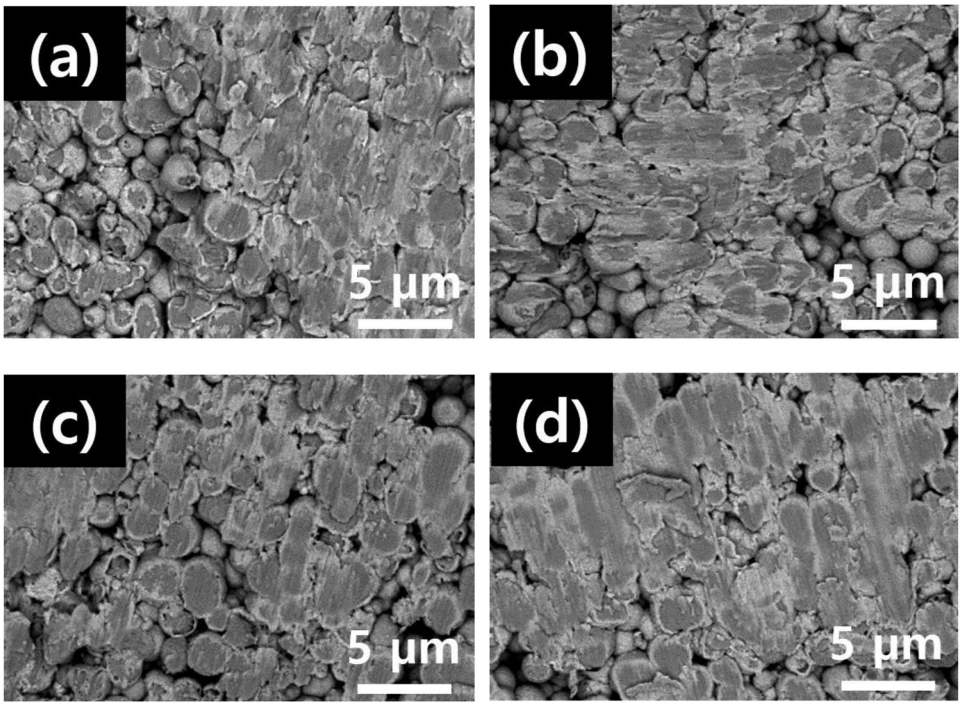

Figure 14. BSE images showing fracture surfaces of bondlines fabricated at 250°C using 40 wt-% Ag-coated Cu particles for different bonding times: (a) 0.5, (b) 1, (c) 5 and (d) 10 min.

Ag nodules on the particle surfaces, which caused sintering between Ag-coated Cu particles and was beneficial for the bonding. Thus, the sinter-bonding speed was significantly high. Consequently, sufficient shear strengths of 24.6 and 34.1 MPa were measured even after rapid bonding for 1 min at 220 and 250°C, respectively, when the Ag coating content was 20 wt-%. When the Ag coating content was increased to 40 wt-%, high shear strengths of 29.5–30.5 and 35.6–36.3 MPa were obtained even after extremely short bonding times of 0.5–1 min at 220 and 250°C, respectively. In addition, near-full-density bondlines could be attained after the short bonding time of 5 min at both 220 and 250°C, which resulted in tremendously increased shear strengths of 55.2 and 68.4 MPa. This very rapid formation of high-density

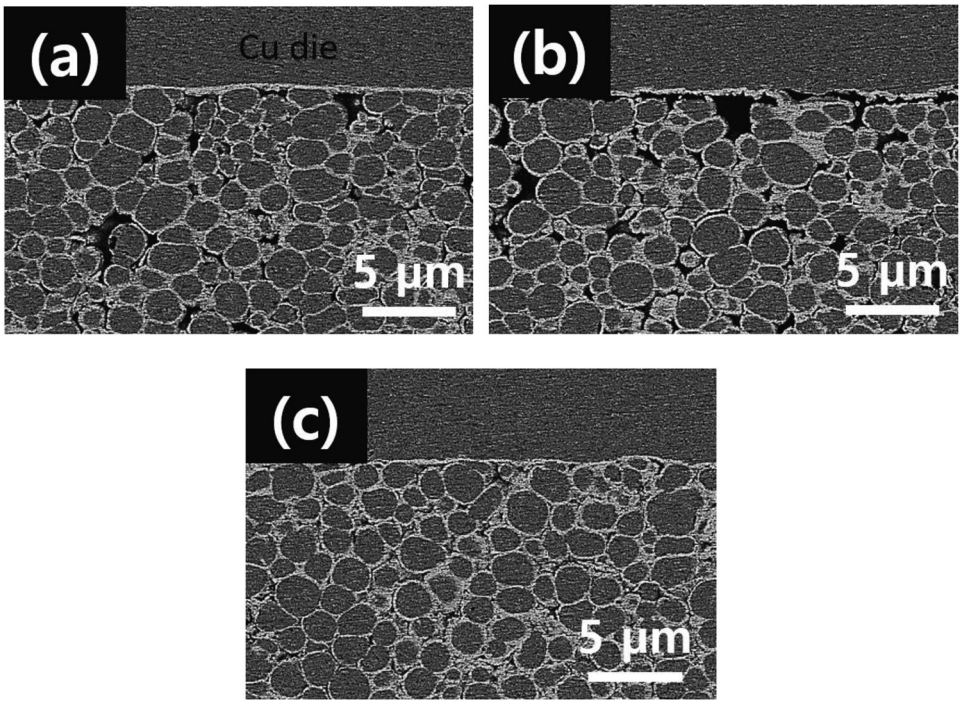

Figure 15. Cross-sectional bondline BSE images of Ag-finished dies sinter-bonded at 220°C for 5 min using 40 wt-% Ag-coated Cu particles under different external pressures: (a) 50, (b) 60 and (c) 70 MPa.

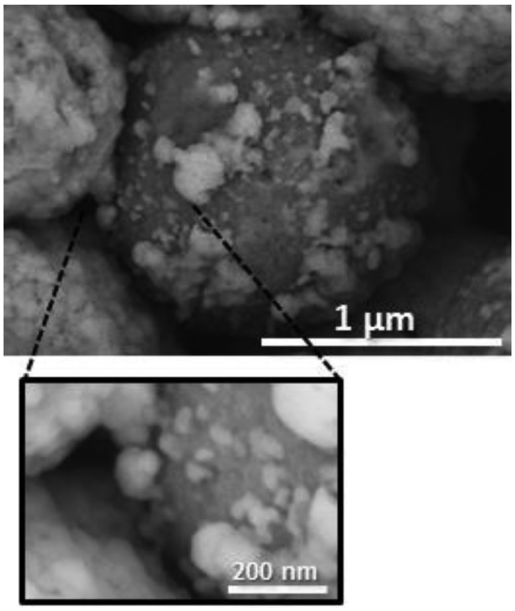

Figure 16. Magnified BSE image showing the formation of nano-nodules by dewetting of Ag shells and the Ag to Ag sintering during heating at 250°C.

bondline structure could be explained by invoking a nano-volcanic eruption behaviour of thick Ag shells.

Disclosure statement

No potential conflict of interest was reported by the author(s).

Funding

This research was funded and conducted under 「the Competency Development Program for Industry Specialists」 of the Korean Ministry of Trade, Industry and Energy (MOTIE), operated by Korea Institute for Advancement of Technology (KIAT) (No. P0002092, HRD program for Development of Advanced Designers for Highly-reliable Mechanical Components).

Notes on contributors

Sung Yoon Kim graduated as a master of materials science and engineering from the Seoul National University of Science and Technology. He mainly researched the high-speed sinter-bonding using silver-coated copper particles.

Eun Byeol Choi is a PhD candidate in a program of materials science and engineering of a convergence institute of biomedical engineering and biomaterials at the Seoul National University of Science and Technology. She is mainly researching the high-speed sinter-bonding using copper fractal particles.

Dong-Hyun Joo is a PhD candidate in a convergence institute of biomedical engineering and biomaterials at the Seoul National University of Science and Technology. His main research interest is miniaturised medical systems, MEMS packaging and MEMS applications.

Jong-Hyun Lee is a professor in a department of materials science and engineering at the Seoul National University of Science and Technology. His main research interest is powder synthesis, solder and sinter-bonding, and electronic packaging technology.

ORCID

Jong-Hyun Lee http://orcid.org/0000-0002-3792-0404

References

[1] Abtew M, Selvaduray G. Lead-free solders in microelectronics. Mat Sci Eng R. 2000;27(5–6):95–141.
[2] Lalena JN, Dean NF, Weiser MW. Experimental investigation of Ge-doped Bi-11Ag as a new Pb-free solder alloy for power die attachment. J Electron Mater. 2002;31(11):1244–1249.
[3] Kim S-J, Kim K-S, Kim S-S, et al. Characteristics of Zn-Al-Cu alloys for high temperature solder application. Mater Trans. 2008;49(7):1531–1536.
[4] Suganuma K, Kim SJ, Kim KS. High-temperature lead-free solders: properties and possibilities. JOM. 2009;61(1):64–71.
[5] Chin HS, Cheong KY, Ismail AB. A review on die attach materials for SiC-based high-temperature power devices. Metall Mater Trans B. 2010;41(4):824–832.
[6] Chidambaram V, Hattel J, Hald J. High-temperature lead-free solder alternatives. Microelectron Eng. 2011;88(6):981–989.
[7] Zeng G, McDonald S, Nogita K. Development of high-temperature solders: Review. Microelectron Reliab. 2012;52(7):1306–1322.
[8] Kotadia HR, Howes PD, Mannan SH. A review: on the development of low melting temperature Pb-free solders. Microelectron Reliab. 2014;54(6–7):1253–1273.
[9] Yang TL, Wu JY, Li CC, et al. Low temperature bonding for high temperature applications by using SnBi solders. J Alloy Compd. 2015;647:681–685.
[10] Zhu ZX, Li CC, Liao LL, et al. Au-Sn bonding material for the assembly of power integrated circuit module. J Alloy Compd. 2016;671:340–345.
[11] Park SW, Nagao S, Kato Y, et al. Quasi-transient liquid-phase bonding by eutectic reaction of Sn-plated Zn on Cu substrate for high-temperature die attachment. J Alloy Compd. 2015;637:143–148.
[12] Zhang Z, Lu GQ. Pressure-assisted low-temperature sintering of silver paste as an alternative die-attach solution to solder reflow. IEEE Trans Electron Packag Manuf. 2002;25(4):279–283.
[13] Wang T, Chen X, Lu G-Q, et al. Low-temperature sintering with nano-silver paste in die-attached interconnection. J Electron Mater. 2007;36(10):1333–1340.
[14] Khazaka R, Mendizabel L, Henry D. Review on joint shear strength of nano-silver paste and its long-term high temperature reliability. J Electron Mater. 2014;43(7):2459–2466.
[15] Siow KS. Are sintered silver joints ready for use as interconnect material in microelectronic packaging? J Electron Mater. 2014;43(4):947–961.
[16] Jiu J, Zhang H, Nagao S, et al. Die-attaching silver paste based on a novel solvent for high-power semiconductor devices. J Mater Sci. 2016;51(7):3422–3430.
[17] Paknejad SA, Mannan SH. Review of silver nanoparticle based die attach materials for high power/temperature applications. Microelectron Reliab. 2017;70:1–11.

[18] Zhang H, Chen C, Jiu J, et al. High-temperature reliability of low-temperature and pressureless micron Ag sintered joints for die attachment in high-power device. J Mater Sci: Mater Electron. 2018;29(10):8854–8862.
[19] Siow KS, Lin YT. Identifying the development state of sintered silver (Ag) as a bonding material in the microelectronic packaging via a patent landscape study. J Electron Packag. 2016;138(2):020804.
[20] Morisada Y, Nagaoka T, Fukusumi M, et al. A low-temperature pressureless bonding process using a trimodal mixture system of Ag nanoparticles. J Electron Mater. 2011;40(12):2398–2403.
[21] Kiełbasiński K, Szałapak J, Jakubowska M, et al. Influence of nanoparticles content in silver paste on mechanical and electrical properties of LTJT joints. Adv Powder Technol. 2015;26(3):907–913.
[22] Siow KS. Mechanical properties of nano-silver joints as die attach materials. J Alloy Compd. 2012;514:6–19.
[23] Zhang Z, Chen C, Yang Y, et al. Low-temperature and pressureless sinter joining of Cu with micron/submicron Ag particle paste in air. J Alloy Compd. 2019;780:435–442.
[24] Choi EB, Lee J-H. Dewetting behavior of Ag in Ag-coated Cu particle with thick Ag shell. Appl Surf Sci. 2019;480:839–845.
[25] Grouchko M, Kamyshny A, Magdassi S. Formation of air-stable copper-silver core-shell nanoparticles for inkjet printing. J Mater Chem. 2009;19(19):3057–3062.
[26] Muzikansky A, Nanikashvili P, Grinblat J, et al. Ag dewetting in Cu@Ag monodisperse core-shell nanoparticles. J Phys Chem C. 2013;117(6):3093–3100.
[27] Bochicchio D, Ferrando R. Morphological instability of core-shell metallic nanoparticles. Phys Rev B. 2013;87(16):165435–165464.
[28] Tsai CH, Chen S-Y, Song J-M, et al. Thermal stability of Cu@Ag core-shell nanoparticles. Corros Sci. 2013;74:123–129.
[29] Lee CH, Choi EB, Lee J-H. Characterization of novel high-speed die attachment method at 225 °C using submicrometer Ag-coated Cu particles. Scr Mater. 2018;150:7–12.
[30] Lin S, Nagao S, Yokoi E, et al. Nano-volcanic eruption silver. Sci Rep. 2016;6:34769.
[31] Chen C, Suganuma K. Microstructure and mechanical properties of sintered Ag particles with flake and spherical shape from nano to micro size. Mater Des. 2019;162:311–321.
[32] Chen C, Kim D, Wang Z, et al. Low temperature low pressure solid-state porous Ag bonding for large area and its high-reliability design in die-attached power modules. Ceram Int. 2019;45(7):9573–9579.
[33] Johnson CA. Generalization of the Gibbs-Thomson equation. Surf Sci. 1965;3(5):429–444.
[34] Buffat P, Borel JP. Size effect on the melting temperature of gold particles. Phys Rev A. 1976;13(6):2287–2298.
[35] Zhao SJ, Wang SQ, Cheng DY, et al. Three distinctive melting mechanisms in isolated nanoparticles. J Phys Chem B. 2001;105(51):12857–12860.
[36] Maruyama M, Matsubayashi R, Iwakuro H, et al. Silver nanosintering: a lead-free alternative to soldering. Appl Phys A. 2008;93(2):467–470.